8

The Effects of Adolescent Alcohol Exposure on Stress-Related Pathways and Behaviors

Taylor Collins, Ben Litchfield, Chelsea Kasten, Eleanor Holmgren, Tiffany Wills.
Louisiana State University Health Sciences Center, Department of Cell Biology and Anatomy, New Orleans, LA.

Introduction

- Individuals who consume alcohol as adolescents have an increased risk of developing alcohol use disorder, but the mechanisms leading to increased vulnerability are unknown.
- The BNST is involved in stress and negative affect induced alcohol relapse.

Previous work using a mouse model of intermittent alcohol vapor (AIE) demonstrated that adolescent alcohol enhances glutamate release and plasticity in the bed nucleus of the stria terminalis (BNST).

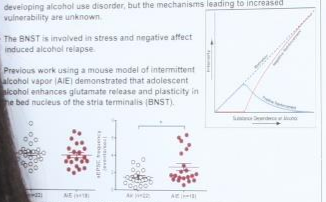

...testing the hypothesis that adolescent alcohol exposure activates ...volved in stress/ fear-related circuitry and produces long term ...ail- fear conditioning.

Methods

...L6J mice were exposed to two four-day cycles of 16 hrs. ...vapor chambers with 8hrs. of withdrawal, separated by ...turbed days.

...subset of mice were injected with Green ...which tag neurons in brain regions that project to the ...fused 4-6 hrs. after acute withdrawal from AIE. ...hemistry was performed to identify co-labeling of ...early gene cFos and cells labeled with tracer.

...t of mice were also exposed to AIE and then ...amily consume alcohol in an intermittent two ...adigm (escalating to 20% ethanol for 4 weeks).

...r only period, mice were tested in contextual ...ice received 6 low intensity (.4 mA, 1 sec) ...ed with a context. The amount of time spent ...ether the shocks, as well as anxiety-like activity ...pen field prior to shock, is recorded.

...meline

BNST Circuitry

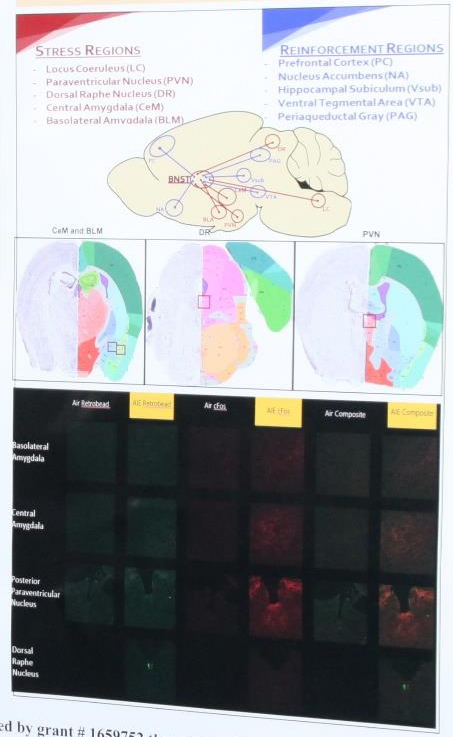

Contextual Fear Conditioning

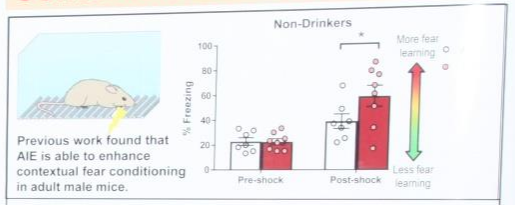

Previous work found that AIE is able to enhance contextual fear conditioning in adult male mice.

Voluntary alcohol drinking following AIE eliminates the enhanced fear conditioning seen in previous AIE experiments. The % freezing was not correlated with voluntary ethanol intake.

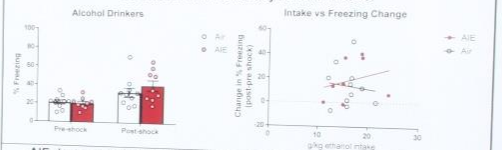

AIE does not alter basal anxiety levels. The level of anxiety activity was not correlated with voluntary ethanol intake.

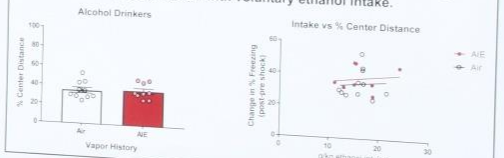

Discussion

- Retrobeads were only strongly expressed in the dorsal raphe nucleus
  - This largely serotonergic-projecting region has been implicated in depression & negative affect
  - Lack of retrobeads in other regions may be due to the use of a small, unilateral bolus
- AIE mice had extensive cFos in stress regions during withdrawal
  - This enhanced activity during withdrawal may contribute to a heightened fear response
- Enhanced fear activity is normalized by voluntary ethanol intake.
  - Voluntary ethanol intake following AIE withdrawal may normalize increased activity in regions associated with stress and fear.

...esearch project was supported by grant # 1659752 through the National Science Foundation (NSF) and NIAAA (K99/R00 AA022651), Research Experiences for Undergraduates (REU) Program

15

Estrogenic Regulation of Lysyl Oxidase in Cardiac Fibroblasts

Tiérra Foley, Nicholas Fried, Dr. Jason Gardner
Department of Physiology, Louisiana State University Health Sciences Center

LSU Health NEW ORLEANS School of Medicine

NSF

Background

According to the American Heart Association's 2019 update, heart disease remains the number one cause of death in the United States, accounting for approximately 363,452 deaths in 2016 and costing 218.7 billion dollars annually. Although cardiac disease is the leading cause of death in both men and women, women develop heart disease ten years later than men. Yet, after menopause, the incidence of heart disease in women is similar to men, suggesting that estrogen may play a part in premenopausal cardioprotection. Previously, the Gardner lab found that ovariectomized rats lost the cardioprotective effects demonstrated by intact females. Adverse cardiac remodeling was associated with high lysyl oxidase (LOX) expression and activity in male rats, with mortality rates of 24.5% in males to 2.5% in females, after 8 weeks of volume overload stress.

Hypothesis

downregulates lysyl oxidase (LOX) and expression through the TGF-β pathway.

Methods

The cardiac fibroblast cells were collected from 10-wk old, female, Sprague-Dawley rats. Once collected the cells were stored in Dulbecco's Modified Eagle Medium (DMEM). The cells were defrosted, plated, and passaged until they reach P3. At this point, the cells were divided into 4 treatment groups: estrogen, PPT (α agonist), DPN (β agonist), and vehicle (DMSO). Cells were plated into a sixty-millimeter dishes, each dish contained 800,000 cells. Each treatment had a concentration of 10 nM. After 24 hours, the media was collected.

Amplite assay tested the media for LOX activity by using a LOX substrate that forms peroxide as LOX oxidizes. The rate of oxidation is detected using the Amplite HMP substrate and responds with increasing fluorescence that is recorded by a microplate reader.

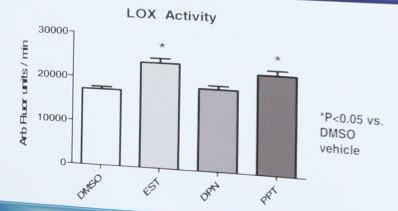

Interpretation

In the presented activity data, we have shown that there is a significant increase in LOX activity with estrogen treatment. Specific agonism of alpha and beta estrogen receptors with PPT and DPN respectively demonstrates that LOX regulation by estrogen is via the alpha estrogen receptor. With the introduction of estrogen, LOX activity increases 38% ($p < 0.05$) in comparison to the control (DMSO).

Ongoing Experiments

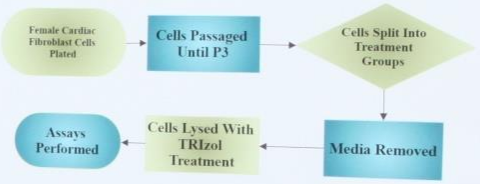

The cardiac fibroblast cells were collected from 10-wk old, female, Sprague-Dawley rats. Once collected the cells were stored in Dulbecco's Modified Eagle Medium (DMEM). The cells were defrosted, plated, and passaged until they reach P3. At this point, the cells were divided into 5 treatment groups: estrogen, TGFβ, estrogen + TGFβ, estrogen + TGFβ antagonist (SB505124), and vehicle (DMSO). Cells were plated into six well plates with a seeding density of 75,000 cells/plate. TGFβ and TGFβ antagonist had a treatment concentration of 10μM, while estrogen had a treatment concentration of 10 nM. After 12 hours, the cells were harvested, lysed, and the media was collected.

The lysed cells will be tested using qPCR analysis of fibroblast lysates for relative expression of mRNA. The housekeeping gene RPS13 is used to compare relative quantifications.

Conclusion

LOX activity is elevated with estrogen treatment, and this elevation is specifically mediated by alpha estrogen receptor agonism. Our hypothesis will be rejected either in part or in totality pending qPCR results of LOX expression.

This research project was supported by grant # 1659752 through the National Science Foundation (NSF), Research Experiences for Undergraduates (REU) Program

NATIONAL INSTITUTES OF HEALTH

17

18

Construction of a short-lived fluorescent protein genetic reporter.

LSU Health NEW ORLEANS School of Medicine

Hassan A. Hassan[1], Li Shen MD, PhD[2].

Xavier University of Louisiana, New Orleans, LA.[1]

Department of Microbiology, Immunology, & Parasitology, LSU Health Science Center, New Orleans, LA.[2]

Abstract

Studies of the unique chlamydial developmental cycle and gene expression have been greatly facilitated by recent success in the development of fluorescence protein reporter gene using transformation of *C. trachomatis* with a plasmid. This powerful tool allows to directly visualize dynamic growth of *Chlamydia in situ* in individual living cells. We have shown that a red-shift green fluorescence protein driven by a chlamydial *ompA* promoter has a half live of ~3 hours in a transformed *C. trachomatis* LGV L2 strain under the condition that results in a productive infection. An ideal reporter gene of temporal transcription programs includes a short half-life that avoids extended accumulation when transcription is turning off. In an effort to meet this criterion, here, we adapted a GFP variant designated as GFP[LVA] which contained a short peptide sequence to the C-terminal end of intact GFP and rendered GFP's sensitivity to the action of endogenous tail-specific protease, tsp, in *E. coli*. *C. trachomatis* encodes a homologue of Tsp. To test the hypothesis that proteolytic degradation of GFP[LVA] is a conserved trait in *C. trachomatis*, we constructed a new reporter plasmid pCtGFP[LVA] for chlamydial transformation. Briefly, *E. coli* strain DH10β cells (New England Biolabs) were used for the molecular cloning. A two-step cloning strategy was used to construct vector pCtGFP[LVA]. First, the pPeuo[LVA]E was constructed by ligation of SpeI/BstBI digested pBC-A1-009 (this vector contains gene encoding GFP[LVA]) and the SpeI/BstBI-elevated fragment from pPvGFP:SW2. The latter fragment carries a chlamydial *euo* promoter flanked by a ribosomal binding site of *tuf* gene. Second, the SpeI and SmaI–digested DNA fragment of pPeuo[LVA]E was inserted into the SpeI-(SalI-blunted)-digested pBOMBeuo. The resultant plasmid pCtGFP[LVA] contains gene coding for GFP[LVA]) under the control of an early promoter from *euo* gene as well as eight open reading frames (ORFs) and an origin of replication from conserved *C. trachomatis* plasmid. This plasmid also contains an *E. coli* origin of replication and a *bla* gene encoding resistance to beta-lactam antibiotics allowing for selection of recombinants with ampicillin. We are presently working on transformation of *C. trachomatis* with pCtGFP[LVA] and determining **1**) what is the half-life in *C. trachomatis*, and **2**) whether the short-lived GFP[LVA] reporter gene could accurately track and predict the transient mRNA profile of the early chlamydial gene, *euo* during infection.

Strains and plasmids used

Cloning Strategy

Figure 1 shows the schematic process of plasmid construction

Map of plasmid

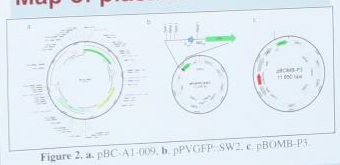

Figure 2. a. pBC-A1-009, **b.** pPVGFP::SW2, **c.** pBOMB-P3.

Agarose gel electrophoresis

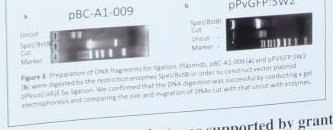

Figure 3. Preparation of DNA fragments for ligation. Plasmids, pBC-A1-009 (**a**) and pPvGFP:SW2 (**b**) were digested by the restriction enzymes SpeI/BstBI in order to construct vector plasmid pPeuo[LVA]E by ligation. We confirmed that the DNA digestion was successful by conducting a gel electrophoresis and comparing the size and migration of DNAs cut with that uncut with enzymes.

Results

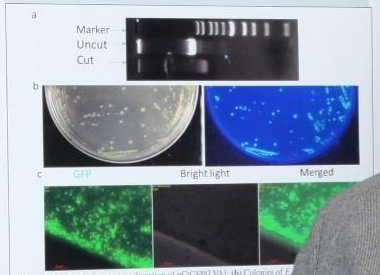

Figure 4. (**a**) restriction enzyme digestion of pCtGFP[LVA]; (**b**) Colonies of *E.* plasmid pCtGFP[LVA] grown on a chloramphenicol-containing LB agar plate exposed (right) to Ultraviolet light. (**c**) analysis of *E. coli* cells carrying pCt microscopy. Images were taken under GFP channel (left) and bright light (m was shown on right.

Sequence of the C-termina

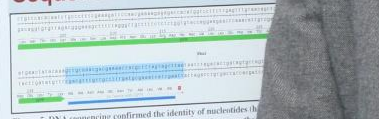

Figure 5. DNA sequencing confirmed the identity of nucleotides (b gene in pCtGFP[LVA]. The relevant amino acids as shown on the

Conclusion and future

- Using molecular cloning technique, we were chlamydial shuttle vector which contains a G
- *E. coli* carrying pCtGFP[LVA] displayed GFP
- We are presently working on transformation of pCtGFP[LVA]
- We will further determine **1**) the half-life of GFP and **2**) whether the this improved reporter gene is transient mRNA profile of the chlamydial *euo* gen

This research project was supported by grant # 1659752 through the National Science F (NSF), Research Experiences for Undergraduates (REU) Program and NIH grant A

References

1. Cong Y, Gao L, Zhang Y, Xian Y, Hua Z, Elaasar H, Shen L. **Quantifying promoter activity during the developmental cycle of Chlamydia trachomatis.** Sci Rep. 2016 Jun 6;6:27244. doi: 10.1038/srep27244.
2. Magaraci MS, Bermudez JG, Yogish D, Pak DH, Mollov V, Tycko J, Issadore D, Mannickarottu SG, Chow BY **Toolbox for Exploring Modular Gene Regulation in Synthetic Biology Training.** *ACS Synth Biol. 2016 Apr 25.*

Identification of Isoform-Specific Intersectin
Human Pathogenic Fungus *Cryptococcus ne*

Haley Hill, Ping Wang.

Department of Microbiology, Immunology, and Parasitology, Louisiana State University Health Orleans, LA, USA

III. Virulence Factors

Figure 3. Virulence Factors of *C. neoformans*. A polysaccharide capsule, melanin, and the secretion of enzymes like urease are critical to virulence.

IV. Homology of Cin1 with ITSN1

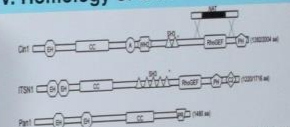

Figure 4. Cin1 shares high sequence homology with human CNS-specific protein ITSN1.

V. Construction of Cin1-L and Cin1-S

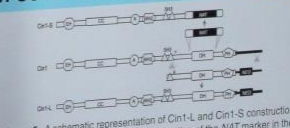

Figure 5. A schematic representation of Cin1-L and Cin1-S construction. Cin1-S was previously obtained by an insertion of the *NAT* marker in the DH-PH. A ~5 kb fragment with a CAG (*) to CAA (#) transition mutation linked to the *NEO* marker gene was obtained for transformation. Sheer symbols mark expected double crossover recombination locations.

esearch project was supported by grant # 1659752 through the National Science Foundation Research Experiences for Undergraduates (REU) Program

VI. Gel E

Figure 6. Obtaine transformants. 10

VII. DNA

Figure 7. DNA Se Mutations. The di transformant that right is DNA sequ and *Cin1-L* allele.

Results

- ✓ The initial 30 wild-type or bo
- ✓ None of the tra
- ✓ The remaining

Conclusi

- ✓ If no JEC21 r transformants
- ✓ Following obta injected into th
- ✓ A murine mod S.
- ✓ Overall, comp understanding and aid in the

References

1. Shen G, Whitting intersectin homo 2010; 76:662-76
2. Wang P, Shen C charting new an

17

18

Identification of Isoform-Specific Intersectin Mutants in Human Pathogenic Fungus *Cryptococcus neoformans*.

LSU Health NEW ORLEANS School of Medicine

Haley Hill, Ping Wang.

Department of Microbiology, Immunology, and Parasitology, Louisiana State University Health Sciences Center, New Orleans, LA, USA

Introduction

Cryptococcus neoformans is a pathogenic fungus that infects immunocompromised and healthy individuals leading to meningoencephalitis. It exhibits the evolutionary advanced ability to penetrate the blood-brain barrier. However, the mechanisms adopted by the fungi to survive in the host central nervous system are unknown. Cryptococcal intersectin 1 (Cin1) has been identified as a novel endocytic protein. Cin1 plays a vital role in intracellular trafficking, which is critical to virulence. Understanding the role Cin1 plays in virulence can lead to the development of life-saving treatment options.

Cin1 is expressed as two isoforms, Cin1-L (long isoform) and Cin1-S (short isoform). Cin1-S displays a survival in a murine model of the CNS, and Cin1-L is the human CNS-specific protein Intersectin 1. that Cin1 and its isoform formation play a role To test this hypothesis, we plan to create a fection in mice and compare it to Cin1-S.

Route

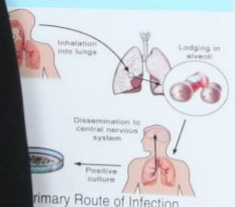

rimary Route of Infection.

ny PCR ification → DNA Sequencing

reening Process of JEC21 Transformants were streaked. y PCR was performed to obtain ts. Lastly, the fragments were ecific point mutations.

III. Virulence Factors

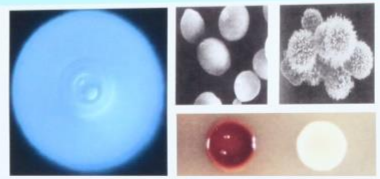

Figure 3. Virulence Factors of *C. neoformans*. A polysaccharide capsule, melanin, and the secretion of enzymes like urease are critical to virulence.

IV. Homology of Cin1 with ITSN1

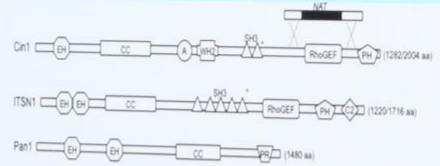

Figure 4. Cin1 shares high sequence homology with human CNS-specific protein ITSN1.

V. Construction of Cin1-L and Cin1-S

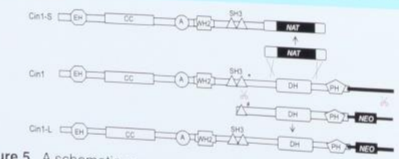

Figure 5. A schematic representation of Cin1-L and Cin1-S construction. Cin1-S was previously obtained by an insertion of the *NAT* marker in the DH-PH. A ~5 kb fragment with a CAG (*) to CAA (#) transition mutation linked to the *NEO* marker gene was obtained for transformation. Sheer symbols mark expected double crossover recombination locations.

VI. Gel Electrophoresis

Figure 6. Obtained PCR fragments following Colony PCR of 11 JEC21 transformants. 10 JEC21 transformants were isolated and sequenced.

VII. DNA Chromatogram

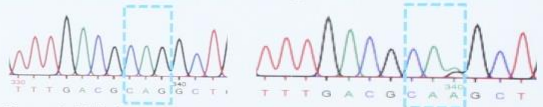

Figure 7. DNA Sequencing of JEC21 Transformants to Identify Point Mutations. The diagram on the left is DNA sequenced from a transformant that displayed the wild-type sequence. The diagram on the right is DNA sequenced from a transformant that displayed the wild-type and *Cin1-L* allele.

Results

- ✓ The initial 30 screened JEC21 transformants displayed either the wild-type or both the wild-type and *Cin1-L* allele.
- ✓ None of the transformants displayed only the *Cin1-L* allele.
- ✓ The remaining 27 JEC21 transformants are being screened.

Conclusion and Future Directions

- ✓ If no JEC21 mutants are identified amongst the 57, then more transformants will be obtained and screened.
- ✓ Following obtainment of JEC21 mutants, the Cin1-L mutants will be injected into the brains of mice.
- ✓ A murine model will be used for the comparison of Cin1-L to Cin1-S.
- ✓ Overall, comparison of the Cin1-S to Cin1-L will yield an improved understanding of the pathogenesis mechanisms of *C. neoformans* and aid in the development of life-saving treatment options.

References

1. Shen G, Whittington A, Song KJ, Wang P. Pleiotropic function of intersectin homologue Cin1 in *Cryptococcus neoformans*. *Mol Micro.* 2010; 76:662-76.
2. Wang P, Shen G. The Endocytic adaptor proteins of pathogenic fungi: charting new and familiar pathways. *Med. Mycol.* 2011; 49:449-57.

This research project was supported by grant # 1659752 through the National Science Foundation (NSF), Research Experiences for Undergraduates (REU) Program

LSU Health NEW ORLEANS School of Medicine

Arginine-170 is Important in Stabilizing the Active Parkin Oligomer

Kariza Hossain, Jennifer Klein, Virginia Ronchi, Oygul Mirzalieva, and Arthur Haas.

Department of Biochemistry & Molecular Biology, Louisiana State University Health Sciences Center, New Orleans, LA

20

Introduction

It is increasingly apparent that the metabolic health of mitochondria is critical to a range of human pathologies including various neurodegenerative and musculoskeletal diseases. Cells harbor multiple pathways for mitochondria quality control that involve the detection and removal of damaged mitochondria and mitochondrial proteins. The major pathway for this targeted degradation of mitochondrial protein components requires the enzymes Parkin and PINK1. Parkin is a relatively non-specific ubiquitin ligase required for the degradation of mitochondrial proteins damaged by oxidative stress (2),(3). PINK1 is a mitochondrial kinase that activates Parkin by phosphorylating the Ser-65 of Parkin (3). Despite considerable advances in understanding Parkin and its relation to the pathogenesis of PD and other diseases, the mechanism of Parkin is not well understood due to the absence of reliable quantitative functional assays for its activity (2). Parkin is an RBR ligase similar in catalytic activity to HECT domain ligases (5). The Haas lab has recently extended previous successes with the HECT domain ligases to RBG ligases, with the current experiments aimed to explore the mechanism of human Parkin conjugation (7). Previous kinetic studies show that Parkin exhibits cooperativity with a Hill value of 2, suggesting that its active form is a dimer. PISA analysis of the Parkin dimer interface revealed an extensive apolar surface (630 Å^2 buried) stabilized by hydrogen bonding to Arg-170 and Lys-220. Experiments were designed to test the hypothesis that the active Parkin dimer is stabilized in part by interactions with the Arg-170 residue.

The 1.79 Å structure of human Parkin (PDB 5C1Z) is shown with the individual domains highlighted (1). The N-terminal ubiquitin-like domain (red) normally occludes the binding site on the Ring1 domain (blue) for the E2~ubiquitin thiolester intermediate. Once the Ser-65 residue on the ubiquitin-like domain is phosphorylated by PINK1, a conformational change allows access to the E2~ubiquitin binding site for subsequent transthiolation of the activated ubiquitin to the active site (Cys-431 present on the Ring2 domain (orange). The later ubiquitin thiolester is thought to be directly transferred to the lysine acceptor on the target protein (not shown).

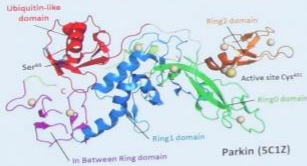

Materials and Methods

The gene for human Parkin (variant 1; accession number BAA25751) was optimized for bacterial codon usage and the resulting synthetic Parkin coding region was subcloned into the Sal1/Not1 sites of the pGEX-4T3-6A expression plasmid. Recombinant GST-Parkin was expressed in *Escherichia coli* BL21 (DE3) cells at 16°C for 14 hours after induction with 0.40 mM IPTG. The resulting protein was purified by affinity chromatography using glutathione Sepharose. GST-Parkin was processed with thrombin and was resolved from processed GST by passage through glutathione Sepharose. The resulting free, unbound Parkin was used in subsequent experiments. A similar approach was used for the generation of GST-PINK1 using the BamH1/Not1 sites of pGEX-4T3-6A, but with the thrombin processing step omitted. Parkin was activated by incubation with GST-PINK1 under optimized conditions in the presence of ATP to phosphorylate the Ser-65 residue of the former. GST-PINK1 was removed by passing the mixture through glutathione Sepharose. Final experiments were designed to test the hypothesis that the active form of Parkin is a dimer stabilized by the Arg-170 residue using biochemically defined kinetic assays (6). Guanidine HCl and labeled ^{125}I-ubiquitin were used in the assays to determine if inhibition of Arg-170 would affect polyubiquitin chain formation.

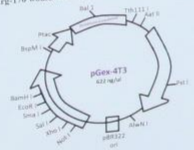

Results

Figure 1. Activation of Parkin by PINK1

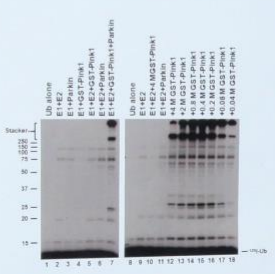

Left Panel - Low Parkin activity (Lane 6) is significantly increased by incubation with PINK1 (Lane 7).
Right Panel – PINK1 concentration dependence for optimal Parkin activity.

Figure 2. Substrate inhibition reveals two E2~ubiquitin binding sites

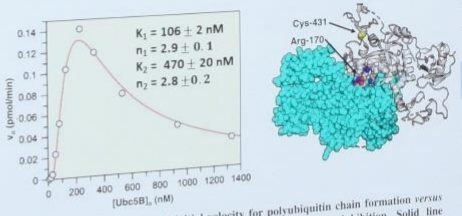

Left Panel – Dependence of initial velocity for polyubiquitin chain formation *versus* Ubc5B concentration showing cooperativity and substrate inhibition. Solid line represents a non-linear regression fit to a cooperative two-site model (7).
Right Panel - Crystal structure for Parkin (5C1Z) rendered in PyMOL showing one subunit in CPK and one in ribbon. Interacting residues are shown in color.

Figure 3. Hyperbolic inhibition of Parkin activity by Guanidine HCl

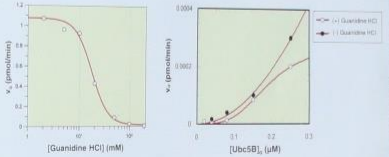

Left Panel - Inhibition of polyubiquitin chain formation as the concentration of Guanidine HCl increases, indicating that Guanidine HCl inhibits Parkin's activity. Solid line represents a non-linear regression fit to a hyperbolic equation.
Right Panel – Comparison of reaction velocity without Guanidine HCl (filled circle) and with Guanidine HCl (open circle). Results suggest Guanidine HCl acts as a mixed inhibitor.

Conclusions

1. Ser-65 phosphorylation alone is sufficient for Parkin activation, contrary to the literature.
2. Substrate inhibition with respect to Ubc5B~ubiquitin requires two substrate binding sites of different affinities and functions, consistent with a Proximal Indexation mechanism for polyubiquitin chain assembly and the presence of unanchored chains (7).
3. Parkin demonstrates allosteric cooperativity with respect to E2~ubiquitin, requiring the active enzyme to be an oligomer. The Hill coefficient suggests the active enzyme is minimally a dimer.
4. PISA analysis identifies the 5C1Z crystal structure of Parkin to be dimeric and stabilized by Arg-170 and Lys-220.
5. Kinetic assays demonstrate Guanidine HCl inhibits Parkin's activity with a K_I of 12 mM, presumably by competing with the Arg-170 residue.

References

1. Kumar, A., Chaugule,V.K., Condos,T.E., Barber,K.R., Johnson,C., Toth,R., Sundaramoorthy,R., Knebel,A., Shaw,G.S., and Walden,H. (2017) Parkin-phosphoubiquitin complex reveals cryptic ubiquitin-binding site required for RBR ligase activity. *Nat. Struct. Mol. Biol.* 24 (5), 475-483.
2. Arkinson,C. and Walden,H. (2018) Parkin function in Parkinson's disease. *Science* 360, 267-268.
3. Pickrell,A.M. and Youle,R.J. (2015) The roles of PINK1, Parkin, and mitochondrial fidelity in Parkinson's disease. *Neuron* 85, 257-273.
4. Haas,A.L. and Siepmann,T.J. (1997) Pathways of ubiquitin conjugation. *Faseb J.* 11, 1257-1268.
5. Spratt,D.E., Walden,H., and Shaw,G.S. (2014) RBR E3 ubiquitin ligases: new structures, new insights, new questions. *Biochem. J.* 458, 421-437.
6. Ronchi, V.P and Haas, A. L. (2012) Measuring rates of ubiquitin chain formation as a functional readout of ligase activity. *Methods Mol.Biol* 832, 197-218.
7. Ronchi, V.P., Kim, E.D., Sawma, C.M., Klein, J.M., and Haas, A.L. (2017) *In silico* modeling of the cryptic E2~ubiquitin binding site of E6-associated protein (EAP)/UBE3A reveals the mechanism of polyubiquitin chain assembly. *J. Biol. Chem.* 292, 18006-18023.

This research project was supported by grant # 1659752 through the National Science Foundation (NSF), Research Experiences for Undergraduates (REU) Program